Chemical exchange and conductivity processes in betaine phosphate and betaine phosphite

1998 J. Phys.: Condens. Matter 10 429

(http://iopscience.iop.org/0953-8984/10/2/022)

J. Phys.: Condens. Matter **10** (1998) 429–443. Printed in the UK PII: S0953-8984(98)85003-0

Chemical exchange and conductivity processes in betaine phosphate and betaine phosphite

P Freude, J Totz, D Michel and M Arndt

Universität Leipzig, Fakultät für Physik und Geowissenschaften, Linnéstraße 5, D-04103 Leipzig, Germany

Received 5 June 1997, in final form 29 September 1997

Abstract. Chemical exchange processes of deuterons in partially deuterated betaine phosphate (DBP) and betaine phosphite (DBPI) crystals are investigated by means of ^{2}H NMR experiments over a wide temperature range. The lineshape analysis of one-dimensional (1D) NMR experiments on DBP reveals a behaviour which is characteristic for exchange processes between all deuterons in the hydrogen bonds. In the temperature range between 230 and 310 K two-dimensional (2D) NMR exchange spectroscopy has been applied, revealing a uniform rate of exchange between all sites. The exchange rates for both crystals are found to show an Arrhenius-like behaviour with activation energies of 83 and 105 kJ mol^{-1}, respectively, where for temperatures above 360 K the rates are obtained from the lineshape analysis of 1D NMR spectra. In addition, conductivity measurements for DBP and DBPI are reported. The dc conductivity in the direction of the quasi-one-dimensional chains, formed essentially by the phosphate and phosphite groups in DBP and DBPI, is characterized by activation energies of 115 and 111 kJ mol^{-1}, respectively. For DBPI this value is close to that obtained for the exchange processes by means of NMR, whereas a difference of about 20 kJ mol^{-1} is found in the case of DBP. Quantitative relations between the exchange and conductivity processes are established and, on the basis of simplifying assumptions, an estimation of effective charge-carrier densities is discussed.

1. Introduction

Betaine phosphate (BP), $(CH_3)_3NCH_2COOH_3PO_4$, and betaine phosphite (BPI), $(CH_3)_3NCH_2COOH_3PO_3$, as well as the respective deuterated compounds (DBP and DBPI) belong to a group of crystals which is composed of the amino acid betaine and an inorganic component. BP and BPI undergo a structural phase transition from a paraelastic high-temperature phase (PE) to an antiferrodistortive phase (AFD) at 365 K and 355 K, respectively. Both crystals possess a monoclinic structure ($P2_1/c$) with four formula units per unit cell. Below 86 K an antiferroelectric ordering occurs in BP, whereas in BPI a ferroelectric behaviour was found below 216 K [1–6]. In BP and BPI as well as in the respective deuterated compounds DBP and DBPI the PO_4^- and PO_3^- tetrahedra are linked by the hydrogen bonds O_4–H_{13}–O_4 and O_6–H_{15}–O_6, thus forming quasi-one-dimensional zigzag chains along the crystallographic *b*-axis [2]. The specification of the deuterium atoms for DBP and DBPI is shown for the case of DBPI in figure 1. The betaine molecules are arranged approximately perpendicularly to the chains and are connected to the phosphate and phosphite tetrahedron by two (O_5–H_{14}–O_1 and O_2–H_{12}–O_3) and one (O_2–H_{14}–O_3) further hydrogen bonds, respectively [2]. In DBPI the fourth deuteron is directly bonded to the phosphorus atom (P–H_{12}) [7].

0953-8984/98/020429+15$19.50

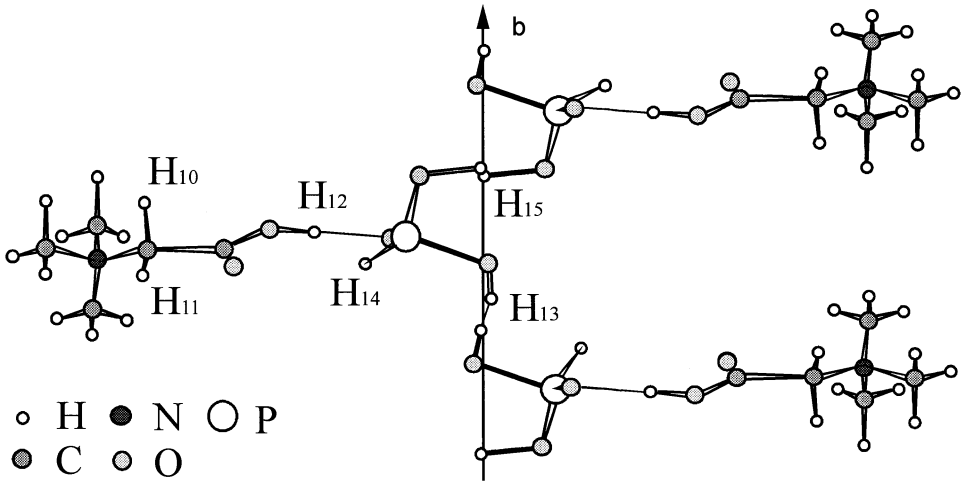

Figure 1. The structure of DBPI in the antiferrodistortive phase. The deuterated lattice sites are indicated for one formula unit.

Magnetic resonance measurements on the deuterated compounds DBP and DBPI were performed to investigate the behaviour of the protons in the hydrogen bonds of BP and BPI [8–11]. Quadrupole-perturbed ^{2}H NMR experiments are a very appropriate tool for investigating the local behaviour of the deuterons due to the direct relationship between the quadrupole line separation $\nu_2 - \nu_1$ and the electric field gradient (EFG) tensor element V_{zz} in the laboratory frame according to

$$\nu_2 - \nu_1 = \frac{6eQ}{4h} V_{zz}^{LAB} = \Phi_{zz}. \tag{1}$$

For the sake of simplicity we use Φ_{zz} (in Hz) instead of V_{zz}. Applying the well-known Volkoff formalism [12], which relates the tensor elements in the crystal frame with the line splitting measured, the EFG tensors in the crystallographic axes system (CAS) were determined for DBP and DBPI [10, 11]. On the basis of this technique the lines in the ^{2}H NMR spectra can be unambiguously ascribed to the various deuterium lattice sites.

In addition to the observed order–disorder phase transition [12, 13], investigations in the temperature range above 300 K revealed typical changes in the one-dimensional (1D) NMR spectra which are characteristic for chemical exchange processes [10]. In the accessible temperature range from 230 to 400 K this corresponds to an inter-H-bond motion whereas, as discussed by Blinc *et al* [14], the intra-H-bond motion is much faster. A detailed study of these (inter-H-bond) exchange processes in DBP and DBPI is achieved by means of one- and two-dimensional (2D) ^{2}H NMR experiments, as will be demonstrated in this paper. To elucidate the role of these processes for the hydrogen (proton, deuteron) conductivity, the results from NMR measurements will be compared with dc-conductivity measurements.

2. Experimental details

The NMR experiments were run at a resonance frequency of 46.073 MHz using a BRUKER MSL 300 NMR spectrometer. An excitation of the complete 1D NMR spectrum was achieved with a pulse duration of 2.5 μs. To avoid the influence of the dead time in the 1D spectra, a quadrupole spin-echo sequence was employed with a pulse distance of 20 μs.

Furthermore, proton decoupling was applied to suppress the broadening of the ^{2}H NMR lines due to dipolar interaction between the deuterons and the remaining protons. The repetition time was chosen between 5 s and 40 s depending on the temperature.

2D ^{2}H NMR exchange experiments were carried out by means of the following echo sequence: $(\pi/2)_x$–t_1–$(\pi/2)_{-x}$–τ_m–$(\pi/2)_x$–τ–$(\pi/2)_y$–τ–t_2. The values t_1, t_2, τ, and τ_m denote evolution time, acquisition time, pulse distance, and mixing time, respectively. A duration of 20 μs was chosen for τ. The phase-cycle sequence used for the four pulses and the receiver phase contained 32 elements in order to reduce errors due to the spectrometer adjustment. Deuterated betaine phosphate crystals were grown from solutions with heavy water. In this process not only a deuteration of the bridging atoms, but also partially a deuteration in the methylene groups of the betaine molecules was achieved.

Measurements of the dielectric permittivity of DBP and DBPI were performed at frequencies from 10^{-2} to 10^5 Hz in the temperature range also covered by the NMR measurements using a Schlumberger Solartron 1255 HF Frequency Response Analyzer. Circularly shaped slices of 0.8 mm thickness and with diameters between 4 and 5 mm, depending on the original crystal shape, were cut from the crystals and evaporated with a thin gold layer. Silver contacts were used for electroding the samples.

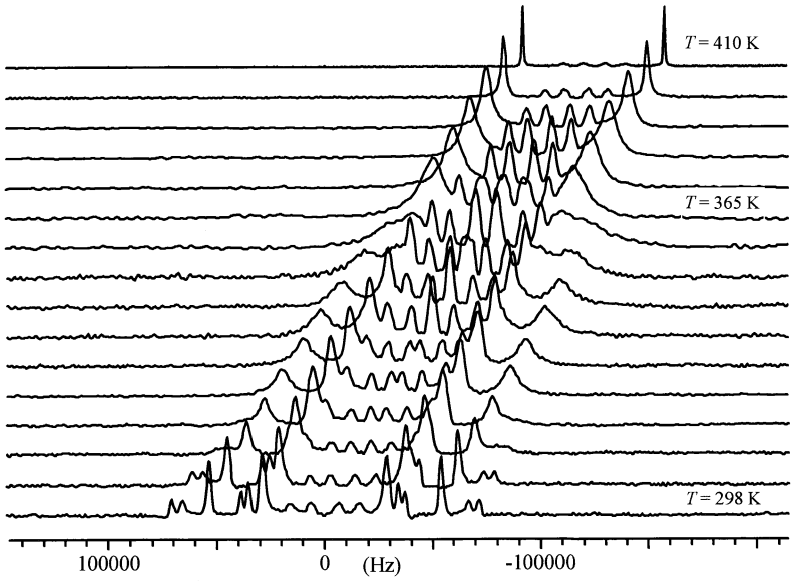

Figure 2. Typical temperature dependence of the quadrupolar line splitting in DBP. The orientation of the crystal was chosen such that the crystallographic *b*-axis is perpendicular to the external magnetic field, and the crystallographic *a*-axis and the direction of the external magnetic field include an angle of 70°. The intensities of the NMR lines are normalized for each spectrum.

3. Results and discussion

3.1. Investigation of the exchange processes in DBP and DBPI

3.1.1. Superposition of the influence of the high-temperature phase transition and exchange processes in the 1D NMR measurements of DBP. In order to separate different influences

on the lineshape and to assign the various deuterium NMR lines to distinct crystallographic sites, temperature-dependent measurements of the 1D ^{2}H NMR spectra were carried out for three different orientations (A1, B1, and B2) of the DBP crystal with respect to the external magnetic field. The orientations A1 and B1 as well as B2 denote a situation where the crystallographic axes *a* and *b* are perpendicular to the external field, respectively. At room temperature, for all of the deuteron sites (H_{12}, H_{13}, H_{14}, and H_{15}) separate line pairs can be observed in the NMR spectra. In a temperature range from $\simeq$320 K up to 400 K, the NMR lines of the deuterons in the hydrogen bonds are broadened and smeared in a typical manner, as shown in figure 2 for the temperature dependence B1. At temperatures above 400 K for all of the deuterons in the hydrogen bonds only one line pair can be observed.

Table 1. Quadrupolar line splittings for three different crystal orientations for DBP for the slow-exchange (columns 2 to 5) and fast-exchange (column 7) limits. In column 6 the values according to equation (2) are given. The line splittings in parentheses were obtained by taking into account the phase transition (see the text).

Temperature dependence	Bond 1: O_5–O_1 / kHz	Bond 2: O_3–O_2 / kHz	Bond 3: O_6–O_6 / kHz	Bond 4: O_4–O_4 / kHz	Weighted frequency / kHz	Observed frequency / kHz
A1	+ 121	+ 64.2	−36.4	−25.2	+ 51.4	+ 48.8
Molecule A	(114.4)	(69.6)	(−102.8)	(25.4)	(48.4)	
A1	+ 107.6	+ 74.8	+ 76	−169.4	+ 45.2	+ 48.8
Molecule B	(114.4)	(69.6)	(25.4)	(−102.8)	(48.4)	
B1	−222.0	−133.2	−15.6	+ 80.6	−107.6	−110.4
Molecule A/B	(−222)	(−133.2)	(32.4)	(32.4)	(−107.7)	
B2	−107.4	−56.4	−144.5	+ 78.2	−65.6	−65.8
Molecule A/B	(−107.4)	(−56.4)	(−33.2)	(−33.2)	(−65.6)	

The line splittings at room temperature and at 400 K are summarized in table 1 for three crystal orientations. In the case of the orientation A1 two formula units (denoted by A and B) can be distinguished. This can be understood in terms of the symmetry properties of the crystal and the special conditions for the quadrupolar-perturbed NMR experiment. Although, in principle, NMR experiments cannot distinguish between a positive or negative sign of the EFG tensor, the relations between the tensor elements are well determined. Due to the inversion invariance of the NMR experiment and due to the occurrence of an inversion centre in the crystal, only two formula units (out of the four formula units present in the AFD phase) are spectroscopically distinguishable. This is realized in case A1. In contrast to the measurements A1, only half of the number of lines can be found in the NMR spectra for the cases B1 and B2. Here in addition to the inversion centre there is a glide plane. The tensor elements V_{zz}, V_{xx}, and V_{xz}, which are observed in the orientation where the *b*-axis is perpendicular to the external magnetic field, are not changed by the glide plane. Thus, the two kinds of molecule possess the same line positions in this orientation as observed experimentally.

For the further interpretation of the observed NMR spectra the broadening of the NMR lines with increasing temperature and the subsequent considerable reduction in the number of line pairs is an important fact. These effects give strong hints as to the presence of processes of exchange between the deuterons in the hydrogen bonds of DBP. The description of the influence of processes of exchange between *n* sites on the one-dimensional NMR spectra is

based on the well-known theory (cf. e.g. Abragam [15]) according to which the lineshape can be calculated by means of the formula

$$I(\omega) = \mathrm{Re}\{\boldsymbol{n}_0 \mathbf{A}^{-1}\mathbf{1}\} \qquad \text{with } \mathbf{A} = \mathrm{i}(\mathbf{w} - \omega\mathbf{E}) + \mathbf{p}^{\mathrm{T}}. \tag{2}$$

In this equation $\mathbf{w}$ denotes the diagonal matrix with the eigenvalues ω_i of the frequency splittings, where i stands for the lattice site. $\mathbf{E}$ indicates the unit matrix of dimension n, and $\mathbf{1}$ is the unit vector. The vector $\boldsymbol{n}_0$, containing the elements n_{i0}, gives the probability that the system has the frequency ω_i. For a stationary process the vector $\boldsymbol{n}_0$ is independent of time. Since the occupation numbers (calculated per phosphate tetrahedron) of the bridging deuterons in the bonds O_5–O_1, O_3–O_2, O_6–O_6, O_4–O_4 are given by the values 1, 1, $\frac{1}{2}$, and $\frac{1}{2}$, the quantities n_{i0} are $(\frac{1}{3}, \frac{1}{3}, \frac{1}{6}, \frac{1}{6})$ for the system under study, respectively.

The rate matrix $\mathbf{p}$ consists of the probabilities p_i of transitions from site j to site i. This matrix results from the description of exchange processes according to the following master equation:

$$\frac{\mathrm{d}n_i}{\mathrm{d}t} = -\sum_{j\neq i}^{n} p_{ji} n_i + \sum_{j\neq i}^{n} p_{ij} n_j a. \tag{3}$$

With the definition

$$p_{ii} = -\sum_{j\neq i}^{n} p_{ji} \tag{4}$$

one obtains

$$\frac{\mathrm{d}n_i}{\mathrm{d}t} = \sum_{j}^{n} p_{ij} n_j \tag{5a}$$

or in matrix notation

$$\dot{\boldsymbol{n}} = \mathbf{p}\boldsymbol{n}. \tag{5b}$$

In addition, the condition of detailed balance has to be taken into account for the case of thermal equilibrium, for which we find

$$\frac{\mathrm{d}n_i}{\mathrm{d}t} = 0 \Rightarrow \sum_{j}^{n} p_{ij} n_{j0} = 0. \tag{6}$$

In the limit of exchange rates much less than the quadrupolar line splitting, the observed lines are not significantly affected by the exchange processes. When the exchange rates are much larger than the line splittings, i.e. for the high-temperature case, typical averaged quadrupole line splittings are observed, which may be simply evaluated as the weighted sums of the static lines, being observed without exchange, with the use of the weight factors n_{i0}.

The experimentally determined splittings and those calculated in this way for higher temperatures are given in table 1. In the case of the measurement A1, slight deviations from the experimental values occur. This can be explained by additional changes due to the phase transition in DBP at 365 K and the temperature dependence of the static frequencies of the lines below 365 K due to the influence of internal vibrations. Thus, for DBP (as well as for DBPI which will be discussed later) the previous conclusions about an order–disorder behaviour could be confirmed again by inspecting the frequency changes over a wide range of temperatures [10, 13]. The temperature dependence of the line splitting is found to be proportional to $\Delta\nu \propto |T - T_c|^{\beta}$ with the exponent $\beta = 0.25$ already measured in NMR investigations on the deuterated CH_2 groups of DBP [13].

The EFG tensor measured at higher temperatures should reflect the influence of the exchange and of the phase transition. First of all, by taking into account the phase transition, we obtain the EFG tensors in the PE phase by arithmetically averaging the respective tensors of the sites H_{12A} and H_{12B}, H_{14A} and H_{14B}, H_{13A} and H_{15B}, and H_{15A} and H_{13B}, i.e. when measured at temperatures below the phase transition. Secondly, we consider the fast-exchange process, according to which the weighted sum has to be calculated. Thus, the EFG tensor V_{av} observed at higher temperatures and the EFG tensors of the deuterons in the hydrogen bonds determined at room temperature (far below the phase transition and in the slow-exchange regime) should obey the following relation:

$$V_{av} = \frac{1}{6}(V_{12A} + V_{12B} + V_{14A} + V_{14B}) + \frac{1}{12}(V_{13A} + V_{13B} + V_{15A} + V_{15B}). \tag{7}$$

The first index (12 to 15) in the EFG tensor characterizes the lattice site whereas the second one (A/B) denotes the molecule observed. The comparison of the two tensors (see reference [11]) reveals a good agreement. This again strengthens the assumption of a process of fast exchange between all deuterons in the hydrogen bonds at the phosphorus tetrahedron. The slight deviations are supposed to be due to further temperature dependencies of the EFG tensors, as already mentioned.

In principle, exchange rates at various temperatures can be determined by means of a simulation of the 1D NMR spectra according to equation (2) and the comparison of the linewidths obtained with those derived from the experiment. However, due to the overlap of the twelve line pairs of the DBP spectra (eight lines for deuterons in the hydrogen bonds and four line pairs for the deuterated CH_2 groups) a general lineshape analysis is rather difficult, if further details of the exchange processes are not available from 2D NMR measurements.

3.1.2. Determination of exchange rates for DBP

3.1.2.1. Two-dimensional ^2H NMR experiments at low temperatures. The 1D NMR experiments described above enabled conclusions about exchange processes and the phase transition at higher temperatures to be reached for when the exchange rate is much larger than the quadrupolar splitting. In order to investigate the processes in the case of low exchange rates, i.e. if the exchange rate is much less than the quadrupolar splitting, 2D ^{2}H NMR exchange experiments were performed. A typical 2D ^{2}H NMR exchange spectrum is shown in figure 3 for DBP at 305 K. Typical off-diagonal peaks occur in the spectra at this relatively low temperature (where in the 1D spectra an exchange process is no longer observable) which allow one to study the exchange processes.

Obviously, this process occurs between the deuterium atoms in *all types* of hydrogen bridges. In order to derive a relation between the exchange rates and the peak intensities in the 2D spectra, equation (5) has to be integrated:

$$\dot{\boldsymbol{n}} = \mathbf{p}\boldsymbol{n} \Rightarrow \boldsymbol{n}(t) = \exp(\mathbf{p}t)\boldsymbol{n}_0 = \mathbf{A}(t)\boldsymbol{n}_0. \tag{8}$$

Here $\boldsymbol{n}(t) = \{n_1, \ldots, n_4\}$ is the vector describing the population numbers of the deuterons at the sites 1 to 4 at the time $t = \tau_m$. The vector $\boldsymbol{n}_0 = \{n_{01}, \ldots, n_{04}\}$ contains the respective numbers of deuterons at the sites 1 to 4 at the time $t = 0$, and $\mathbf{A}$ is the exchange matrix with the elements a_{ij}. Taking into account the inequality $T_2 \ll \tau_m \ll T_1$ between the transverse relaxation time T_2, the mixing time τ_m, and the longitudinal relaxation time T_1, which holds for our experiments, no further relaxation effects have to be considered. The intensities I_{ji} observed in the 2D NMR spectra at a mixing time τ_m are then directly proportional to the number of deuterons exchanging from site j to site i, characterized by n_{ij}.

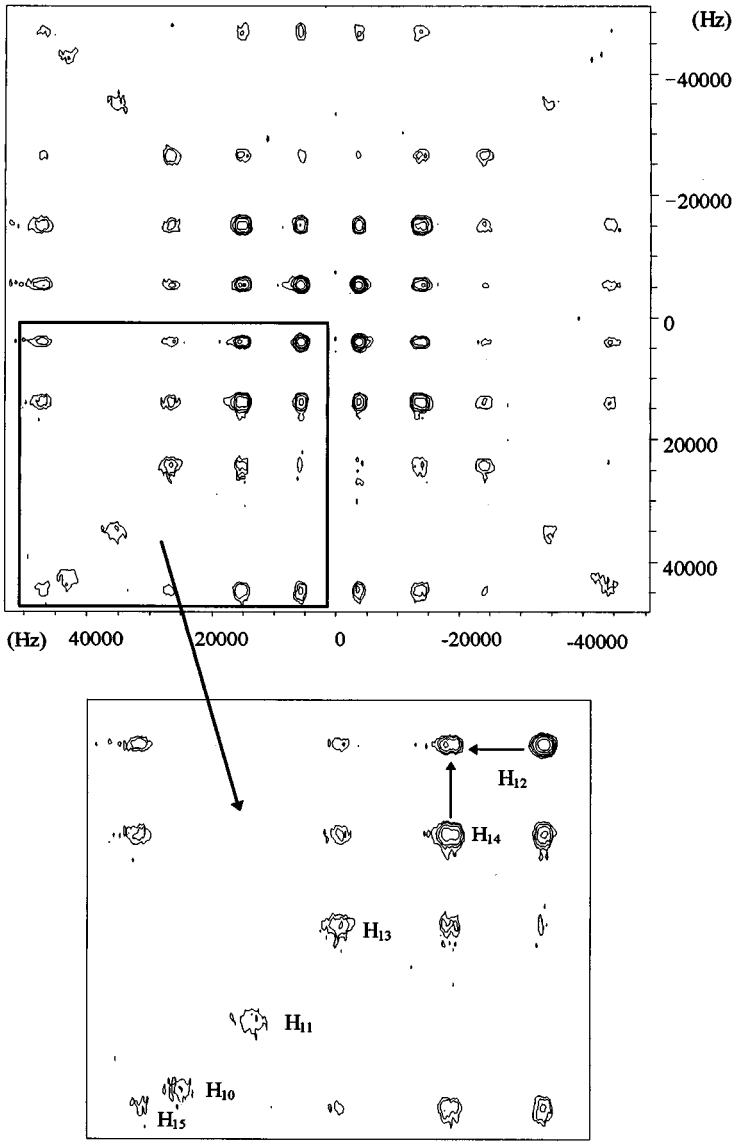

Figure 3. A typical 2D ^{2}H NMR exchange spectrum for DBP at 310 K at a mixing time of 10 ms. The crystallographic *b*-axis is perpendicular to the direction of the external magnetic field. The *a*-axis and the external field include an angle of 41°. The inset shows the lower left-hand part of the spectrum. Exchange processes are characterized by the occurrence of off-diagonal peaks. The off-diagonal peak indicated by two arrows, for instance, reflects the deuteron exchange between sites H_{12} and H_{14}.

For the determination of the rate matrix at a fixed temperature on the basis of the experimentally obtained peak intensities, it is necessary to measure the dependence of these intensities on the mixing time. According to equation (8), the rate matrix for an *n*-site exchange is then fitted to the mixing time dependence of the intensities.

In the case of DBP the rate matrix was determined for three different temperatures

(T = 310 K, 296 K, and 260 K) in the experimentally accessible range of the 2D NMR experiments ($\simeq$230 K to 315 K).

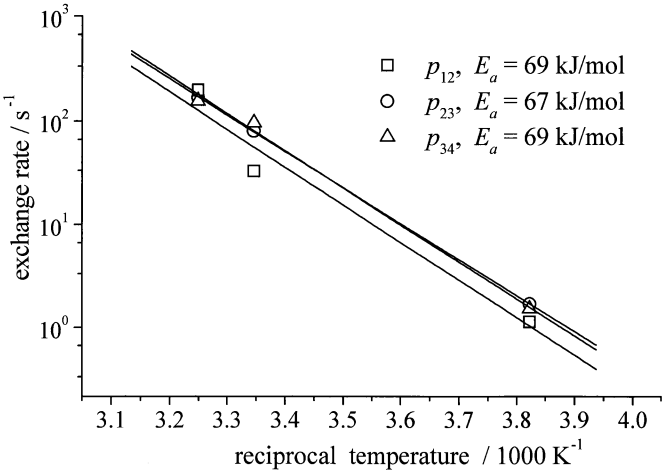

Figure 4. The exchange rates p_{12}, p_{23}, and p_{34} versus the reciprocal temperature for DBP.

Considering the four different sites and having in mind equations (4) and (6), the rate matrix includes six independent elements (p_{12}, p_{13}, p_{14}, p_{23}, p_{24}, and p_{34}). The fitted values of the rates p_{12}, p_{23}, and p_{34} are given in figure 4. Although the data are only available for three different temperatures, the rates were fitted to an Arrhenius equation with an activation energy E_A:

$$p(T) = p_0 \mathrm{e}^{-E_A/RT}. \tag{9}$$

As reflected by approximately equal values for the activation energy E_A and of the pre-exponential factors p_0, the exchange rates p_{ij} show similar behaviour. This implies the assumption of a common exchange rate p, i.e. the simplification that there is only one independent parameter in the rate matrix. As the consequence of this reduction of the number of independent parameters from six to one, the rate matrix can be obtained on the basis of just one 2D NMR spectrum for a fixed temperature. Thus, the time-consuming measurements with different mixing times are avoided.

On the basis of this approach the rate matrix is given by

$$\mathbf{p} = p \begin{pmatrix} -4 & 2 & 2 & 2 \\ 2 & -4 & 2 & 2 \\ 1 & 1 & -6 & 2 \\ 1 & 1 & 2 & -6 \end{pmatrix}. \tag{10}$$

According to equation (8), the following exchange matrix is obtained:

$$\mathbf{A}(t) = \begin{pmatrix} \frac{1}{3} + \frac{2}{3}\mathrm{e}^{-6pt} & \frac{1}{3} - \frac{1}{3}\mathrm{e}^{-6pt} & \frac{1}{3} - \frac{1}{3}\mathrm{e}^{-6pt} & \frac{1}{3} - \frac{1}{3}\mathrm{e}^{-6pt} \\ \frac{1}{3} - \frac{1}{3}\mathrm{e}^{-6pt} & \frac{1}{3} + \frac{2}{3}\mathrm{e}^{-6pt} & \frac{1}{3} - \frac{1}{3}\mathrm{e}^{-6pt} & \frac{1}{3} - \frac{1}{3}\mathrm{e}^{-6pt} \\ \frac{1}{6} - \frac{1}{6}\mathrm{e}^{-6pt} & \frac{1}{6} - \frac{1}{6}\mathrm{e}^{-6pt} & \frac{1}{6} + \frac{1}{2}\mathrm{e}^{-8pt} + \frac{1}{3}\mathrm{e}^{-6pt} & \frac{1}{6} - \frac{1}{2}\mathrm{e}^{-8pt} + \frac{1}{3}\mathrm{e}^{-6pt} \\ \frac{1}{6} - \frac{1}{6}\mathrm{e}^{-6pt} & \frac{1}{6} - \frac{1}{6}\mathrm{e}^{-6pt} & \frac{1}{6} - \frac{1}{2}\mathrm{e}^{-8pt} + \frac{1}{3}\mathrm{e}^{-6pt} & \frac{1}{6} + \frac{1}{2}\mathrm{e}^{-8pt} + \frac{1}{3}\mathrm{e}^{-6pt} \end{pmatrix}. \tag{11}$$

On the basis of experiments at three temperatures, initial values for p_0 and E_A were obtained, which are used in equations (8) and (11) to simulate the dependence of the peak

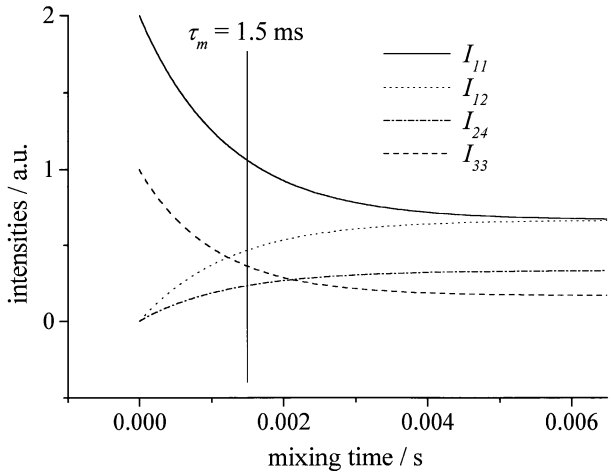

Figure 5. Simulated peak intensities I_{11}, I_{12}, I_{24}, and I_{33} versus the mixing time at $T = 305$ K. For the 2D NMR experiment a mixing time of 1.5 ms was chosen (indicated by the vertical line).

intensities I_{ij} on t for further (fixed) temperatures. For each fixed temperature such a value of the mixing time τ_m in the 2D NMR experiments is chosen for which all peak intensities strongly depend on τ_m (see figure 5).

The exchange rates obtained in this way, i.e. with the approach of a uniform exchange process, were fitted to equation (9), which yielded an activation energy of 82 kJ mol^{-1} (0.85 eV, 9800 K) and a pre-exponential factor of $p_0 = 1 \times 10^{16}$ s^{-1}. The difference with respect to the activation energies obtained for the single rates (as indicated in figure 4) is due the fact that there only three data points were available for the fit. In contrast, the value of 82 kJ mol^{-1} was obtained using a considerably higher number of data points, and therefore can be considered more reliable.

3.1.2.2. One-dimensional ^2H-NMR experiments at high temperatures. On the basis of the approach of a common exchange rate, the 1D NMR spectra were simulated according to equation (2) for different exchange rates. This simulation was carried out for a definite crystal orientation for which the temperature dependence of the 1D NMR spectra had been measured. The aim was to determine the temperature dependencies of the exchange rate in the fast-exchange limit, on the basis of the comparison of the simulated 1D NMR linewidth as a function of the exchange rate and the dependence of the experimentally obtained 1D NMR linewidth on the temperature. The temperature dependence of the exchange rates in the fast-exchange limit again showed a behaviour corresponding to the Arrhenius model. The fit resulted in an activation energy of 78 kJ mol^{-1} and a value of 4×10^{15} s^{-1} for p_0.

These values are in agreement with those found for the slow-exchange limit. The exchange rates in the temperature interval between the two limits could not be determined due to the large number of broadening lines, as mentioned above. However, a fit to the Arrhenius model was carried out for all available exchange rates. This covers a temperature range of 200 K. The results from this fit can be seen in figure 6. Over the whole temperature interval an activation energy of 83 kJ mol^{-1} (0.86 eV) and a value of 2×10^{16} s^{-1} for p_0 were obtained. The accuracy of this plot leads to the conclusion that the assumption of

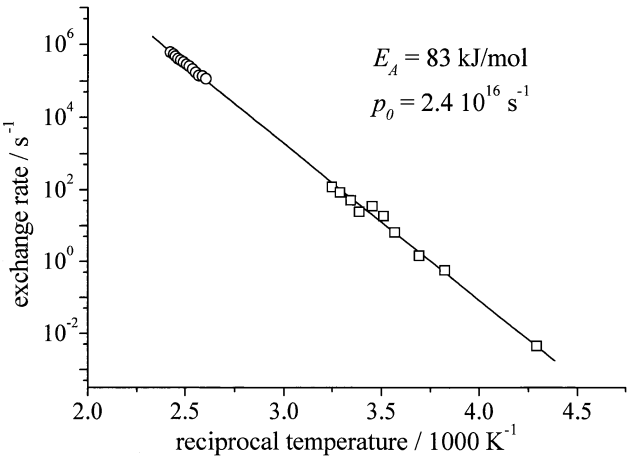

Figure 6. Exchange rates versus reciprocal temperature for DBP for slow and fast exchange (230 K to 430 K) obtained on the basis of a uniform exchange rate for the four sites. The rates in the slow-exchange limit (indicated by □) were obtained by means of 2D ^{2}H exchange NMR; the rates for the fast-exchange limit (indicated by ○) were obtained by comparison of experimentally obtained and simulated 1D linewidths (see the text).

a uniform exchange rate for the four deuterons participating in the exchange process is justified.

3.1.3. Determination of rates of exchange in DBPI. 1D ^{2}H NMR measurements for DBPI gave no direct evidence for chemical exchange processes because apparently no line broadening could be observed in the temperature dependence of the spectra, in contrast to the case for DBP. Thus, fast chemical-exchange processes with exchange rates far above that of the quadrupolar line splitting can be excluded. Considering the structural similarity and the similar behaviour found for DBP and DBPI at higher temperatures [10, 11, 13], exchange processes in DBPI are to be expected. According to the observed 1D NMR spectra these processes have exchange rates which should be small in comparison with the quadrupolar line splitting. In this case the processes should be reflected in 2D ^{2}H exchange NMR measurements. In figure 7 a characteristic 2D ^{2}H NMR spectrum at 310 K is shown. Off-diagonal peaks, indicating exchange processes, occur between the deuterons H_{12}, H_{15}, and H_{13}, i.e. the exchange process involves the deuterons in the hydrogen bonds of DBPI. The deuteron H_{14}, directly bonded to the phosphorus atom, does not show any off-diagonal peaks with the deuterons located in the hydrogen bonds. As represented by the two adjacent diagonal peaks in the 2D NMR spectra, the spectral line ascribed to deuteron H_{14} is split due to the dipolar interaction of the deuteron and the phosphorus nucleus [11]. This interaction causes the off-diagonal peaks of these two lines.

As for DBP, the dependences of the 2D NMR spectra on the mixing time were measured at different temperatures. For each temperature, the rate matrix with a dimension of 3×3 was determined. Here the same procedure as for DBP is applied. The lattice sites labelled 1 to 3 denote the deuterons H_{12}, H_{15}, and H_{13}, respectively. The temperature dependency of the rate matrix is given in figure 8. The activation energies according to equation (10) for the rates p_{12}, p_{13}, and p_{23}, being 99, 107, and 107 kJ mol^{-1}, respectively, are larger than the values obtained for DBP. Again the assumption of a common rate of exchange

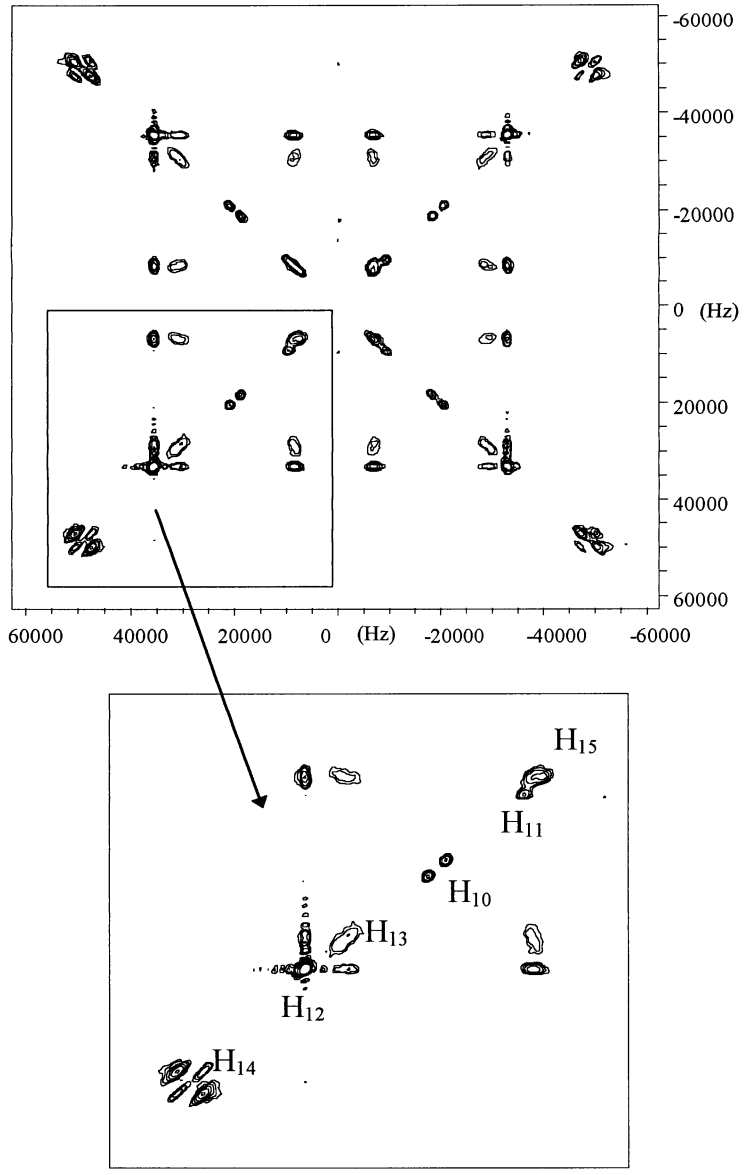

Figure 7. A typical 2D ^{2}H NMR exchange spectrum for DBPI at 310 K at a mixing time of 100 ms. The crystallographic *b*-axis is perpendicular to the external magnetic field. The *a*-axis and the external field include an angle of 76°. The inset shows the upper left-hand part of the spectrum. Exchange processes are characterized by the occurrence of off-diagonal peaks.

between the different sites seems to be justified. Under this condition, $\mathbf{p}$ and the exchange matrix $\mathbf{A}(t)$ are given by

$$\mathbf{p} = p \begin{pmatrix} -2 & 2 & 2 \\ 1 & -4 & 2 \\ 1 & 2 & -4 \end{pmatrix} \tag{12}$$

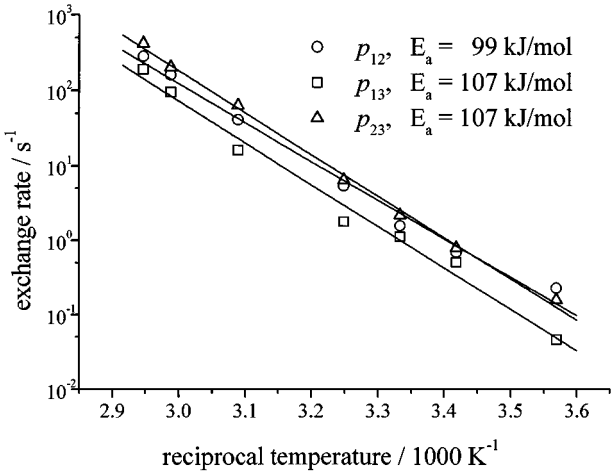

Figure 8. The elements p_{12}, p_{13}, and p_{23} of the rate matrix for DBPI versus the reciprocal temperature.

and

$$\mathbf{A}(t) = \begin{pmatrix} \frac{1}{2} + \frac{1}{2}e^{-4pt} & \frac{1}{2} - \frac{1}{2}e^{-4pt} & \frac{1}{2} - \frac{1}{2}e^{-4pt} \\ \frac{1}{4} - \frac{1}{4}e^{-4pt} & \frac{1}{4} + \frac{1}{2}e^{-6pt} + \frac{1}{4}e^{-4pt} & \frac{1}{4} - \frac{1}{2}e^{-6pt} + \frac{1}{4}e^{-4pt} \\ \frac{1}{4} - \frac{1}{4}e^{-4pt} & \frac{1}{4} - \frac{1}{2}e^{-6pt} + \frac{1}{4}e^{-4pt} & \frac{1}{4} + \frac{1}{2}e^{-6pt} + \frac{1}{4}e^{-4pt} \end{pmatrix}. \tag{13}$$

An activation energy of 105 kJ mol^{-1} (1.09 eV) and a value of $p_0 = 1.4 \times 10^{18}$ s^{-1} were obtained for the common exchange rates. The error in p_0 for our fit can be estimated to be half an order of magnitude; nevertheless its value changes by more than an order of magnitude when not all data points are taken into account in the fit. In order to relate p_0 to vibrational frequencies measured in DBPI [16] one would expect values of approximately 10^{13} s^{-1}, which are significantly smaller than the value of p_0. In this context we would also like to mention investigations on the relationship between the activation energy and the pre-exponential factor [17]. Independently of this, it should be stressed again that the differences in exchange rates between DBP and DBPI as measured by different NMR techniques are beyond the experimental errors as discussed in this context.

On the basis of the temperature dependencies of the exchange rate, the 1D NMR spectra are simulated according to equation (2) for a definite orientation of the DBPI crystal with respect to the external magnetic field for a temperature range above that of the PE phase transition. The orientation was chosen in such a way as to allow us to observe the NMR lineshape for the deuterons H_{12}, H_{13}, and H_{15} separately. The simulated 1D NMR lines for the deuterons H_{13} and H_{15} are broadened above 360 K. For the lines of the deuterons H_{12}, this broadening appears only above 380 K. For temperatures about 400 K one extremely broadened NMR line exists in the NMR spectra for these deuterons. The effect of the broadening of the NMR lines could be observed experimentally for the deuterons H_{12}, H_{13}, and H_{15}. The NMR line splitting was measured for temperatures above 360 K. Unfortunately, the DBPI crystal used in the NMR experiment melted at about 411 K. Hence, the expected averaged NMR line above 425 K was not observable in the 1D NMR experiment.

3.2. Investigation of the conductivity processes in DBP and DBPI

As found for many crystals, the exchange processes of the deuterons (or protons) in a hydrogen bond system are connected to an electrical conductivity. Conductivity measurements and their interpretations have been reported for BP and BPI [18, 19] as well as for other crystals [20, 21]. For DBP and DBPI, due to the quasi-one-dimensional chains parallel to the crystallographic *b*-axis, an anisotropic conductivity can be expected, where the conductivity measured in the direction parallel to the *b*-axis is sufficiently larger than that in a direction perpendicular to the *b*-axis.

The dc conductivity σ_{DC} was measured for different DBP and DBPI samples. For each crystal, two samples were used in which the crystallographic *b*-axis was parallel and perpendicular (the *a*-axis parallel) to the external electric field, respectively. The dc conductivity was obtained from the frequency dependence of the imaginary part (ε') of the dielectric permittivity ε according to equation (14) which is valid for low frequencies [22]:

$$\sigma_{DC} = \varepsilon_0 \varepsilon'' \omega^s. \tag{14}$$

Above 315 K an isolated conductivity wing without any relaxation processes was observed in the dielectric loss (ε'') over a wide frequency range. Furthermore, in this temperature interval the value of the exponent s was found to be $0.97 < s < 1$. Therefore one can be sure that neither ac conductivity nor electrode polarization affected the conductivity data.

Assuming the exchanging (hopping) process of the deuterons to be related to the measured conductivity, the mobility (μ) of the charge carriers used in the equation

$$\sigma_{DC} = nq\mu \tag{15}$$

can be obtained from the Nernst–Einstein equation

$$\mu = \frac{Dq}{kT} \tag{16}$$

Here n is the charge carrier density and D denotes the diffusion coefficient. In the case of a one-dimensional diffusion the value D can be expressed as

$$D = \frac{1}{2} \nu a^2 \mathrm{e}^{-E_A/RT}. \tag{17}$$

Here ν and a stand for the averaged jump frequency and the jump distance of the deuteron motion, respectively. Considering equations (15) to (17), it follows for the dc conductivity that

$$\sigma_{DC} T = \sigma_0 \mathrm{e}^{-E_A/RT} \qquad \text{with } \sigma_0 = nq^2 \nu a^2 / 2k. \tag{18}$$

In equation (18) the charge carrier density n is assumed to be temperature independent. This suggestion will be discussed again in the case of DBP. In figure 9 the fit of the dc conductivities to equation (18) is shown for DBPI and DBP. As expected, the conductivity in the direction of the *b*-axis was found to be three orders of magnitude larger than that in a direction perpendicular to the *b*-axis (not shown here).

The fit according to equation (18) for DBPI over the temperature interval from 320 K to 390 K resulted in values for E_A of 111 kJ mol^{-1} and σ_0 of 1.2×10^{12} K Ω^{-1} m^{-1}. Considering a fitting interval from 320 K to 340 K, for which 2D NMR exchange data are also available, gives $E_A = 105$ kJ mol^{-1} and $\sigma_0 = 1.2 \times 10^{11}$ K Ω^{-1} m^{-1}. This activation energy of the conductivity in the direction of the one-dimensional chains is very close to that found for the exchange processes (105 kJ mol^{-1}). This fact suggests a relationship between the two processes.

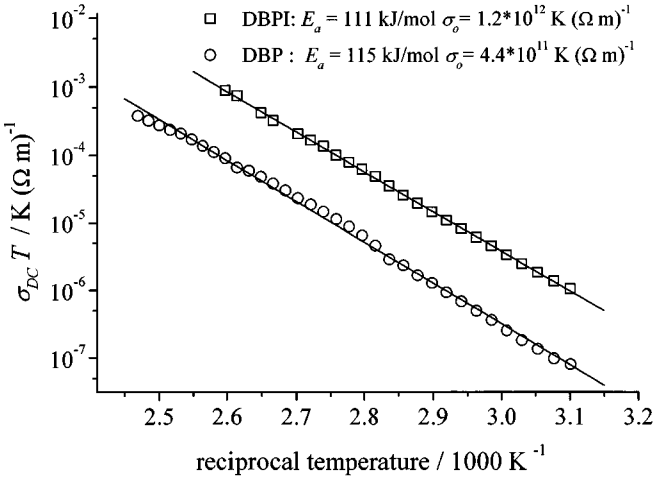

Figure 9. The dc conductivity for DBPI (□) and DBP (○) versus the reciprocal temperature.

For a first rough estimation of the quantity n three simplifying assumptions are made, leading to the interpretation of n as an 'effective' charge-carrier density. Provided first that the conductivity originates from a proton transport along the chains, the charge effectively carried is assumed to be the elementary charge ($q = 1.6\times10^{-19}$ C). Moreover, the value of ν in equation (17) could be interpreted in terms of the pre-exponential factor p_0 obtained from the NMR data (p_0 is multiplied by the factor 2 due to the definition of the exchange rate; see equation (11)). Thirdly, considering the deuterons in the hydrogen bonds to be on average, due to a fast intra-bond exchange, located in the middle of the respective bond, a value of a is derived [10]: it is 3.8 Å. On the basis of these assumptions, the effective charge-carrier density n is calculated to be 2.5×10^{26} m^{-3} which gives a density of 0.2 charge carriers per unit cell. Taking into account different fitting intervals (leading to different values for σ_0) as well as the possibility of determining n at fixed temperatures (using the exchange rate and the conductivity at that temperature), we should mention that the observed charge-carrier densities vary by about an order of magnitude in both directions. It should be stressed again that the calculated 'effective density' is based on the assumption of a transport process of a proton (one positive elementary charge) along the chains according to equation (18).

For DBP the fit over the temperature interval from 320 K to 395 K leads to values for the activation energy of $\sigma_{DC}T$ of $E_A = 115$ kJ mol^{-1} and σ_0 of 4.4×10^{11} K Ω^{-1} m^{-1}. Taking into account a fitting interval at higher temperatures (360 to 395 K) where the influence of relaxation processes on the conductivity fit can be safely excluded, we obtained $E_A = 106$ kJ mol^{-1} and σ_0 of 2.3×10^{10} K Ω^{-1} m^{-1}. The discrepancy between this activation energy and those found for the exchange processes (82 kJ mol^{-1}) is far beyond the experimental error. Hence, in contrast to the case for DBPI, the simplifying assumption of a temperature-independent charge-carrier density has to be dropped.

As a first approach, a thermally activated charge-carrier density $n(T)$ is assumed. According to this assumption, equation (18) should be modified to

$$\sigma_{DC}T = \sigma_0 \mathrm{e}^{-E/RT} = \frac{a^2}{2k} n_0 \nu \mathrm{e}^{-(E_n+E_A)/RT} \tag{19}$$

where E_n stands for the activation energy of the charge-carrier density. The activation energy for $n(T)$ is expected to be equal to the difference in the activation energies of the

conductivity and the exchange process. To check this suggestion, $n(T)$ was calculated for 12 specific temperatures (again using the exchange rate and the conductivity at that temperature, and with a jump distance a of 3.6 Å) and fitted to an Arrhenius law. In this way we find the activation energy E_n to be about 20 kJ mol^{-1} (i.e. corresponding to our expectation), and n_0 is 1.57×10^{27} m^{-3}. In the temperature range covered by our experiments, the densities n of charge carriers were found to be of the same order of magnitude for DBPI and DBP, which suggests similar conductivity behaviours of these crystals. Considering our assumptions, the difference in n should not be overstressed. It should be stressed again, however, that the deviations in the exchange rates for both crystals are far beyond the limits of experimental errors. Further work aimed at achieving a deeper understanding of this fact is in progress.

Acknowledgments

The authors are indebted to Dr A Klöpperpieper and K Kretsch (Saarbrücken) for providing the crystals, and to Professor G Völkel (Leipzig) for helpful discussions. For providing the possibility of performing the conductivity measurements, the authors are indebted to Professor F Kremer (Leipzig). The financial support of the Deutsche Forschungsgemeinschaft is gratefully acknowledged.

References

[1] Albers J, Klöpperpieper A, Rother H J and Ehses K H 1982 *Phys. Status Solidi* a **74** 553
[2] Schildkamp W and Spilker J 1984 *Z. Kristallogr.* **168** 159
[3] Albers J, Klöpperpieper A, Rother H J and Haussühl S 1988 *Ferroelectrics* **81** 27
[4] Schaack G 1990 *Ferroelectrics* **104** 147
[5] Hellenbrand K-H, Ehses K H and Krane H-G 1991 *Z. Kristallogr.* **195** 251
[6] Pöppl A, Völkel G, Metz H and Klöpperpieper A 1994 *Phys. Status Solidi* b **184** 471
[7] Paasch M 1991 *Diploma Work* Universität Mainz
[8] Bauch H, Böttcher R and Völkel G 1993 *Phys. Status Solidi* b **178** K39
[9] Bauch H, Böttcher R and Völkel G 1993 *Phys. Status Solidi* b **179** K41
[10] Freude P and Michel D 1995 *Ferroelectrics* **165** 329
[11] Freude P and Michel D 1996 *Phys. Status Solidi* b **195** 297
[12] Volkoff G M, Petch H E and Smellie D W L 1951 *Phys. Rev.* **84** 602
[13] Freude P, Michel D and Klöpperpieper A 1998 *Ferroelectrics* at press
[14] Blinc R, Dolinsek J and Zalar B 1995 *Solid State Ion.* **77** 97
[15] Abragam A 1961 *Principles of Nuclear Magnetism* (Oxford: Oxford University Press)
[16] Ebert H, Lanceros-Mendez S, Schaack G and Klöpperpieper A 1995 *J. Phys.: Condens. Matter* **7** 9305
[17] Petersson J, Schneider E and Siems R 1980 *Z. Phys.* B **39** 233
[18] Banys J, Klimm C, Völkel G, Böttcher R, Bauch H and Klöpperpieper A 1996 *J. Phys.: Condens. Matter* **8** L681
[19] Hutton S L, Fehst I, Böhmer R, Braune M, Mertz B, Lunkenheimer P and Loidl A 1991 *Phys. Rev. Lett.* **15** 1990
[20] O'Keeffe M and Perrino C T 1967 *J. Phys. Chem. Solids* **28** 211
[21] Kawada A, McGhie A R and Labes M M 1970 *J. Chem. Phys.* **52** 3121
[22] Dyre J C 1988 *J. Appl. Phys.* **64** 2456